Electrochemical and Solid-State Letters, **9** (5) B25-B27 (2006)
1099-0062/2006/9(5)/B25/3/$20.00 © The Electrochemical Society

Porous SOFC Anodes Prepared by Sublimation of an Immiscible Metal Oxide during Sintering

Ying Liu* **and Meilin Liu****,z**

Center for Innovative Fuel Cell and Battery Technologies, School of Materials Science and Engineering, Georgia Institute of Technology, Atlanta, Georgia 30332-0245, USA

Nanostructured composite powder, consisting of 20 wt % SnO_2, 50 wt % NiO, and 30 wt % $Gd_{0.1}Ce_{0.9}O_2$ (GDC), was prepared using a combustion chemical vapor deposition process from a single solution containing all precursors. Bilayer solid oxide fuel cells (SOFC) anodes of different porosity were fabricated by copressing of NiO-GDC powder and SnO_2–NiO-GDC composite powder. Porosity variation in the anodes was achieved by the removal of the SnO_2-phase during firing and subsequent cell testing. Anode-supported SOFC single cells were constructed and tested for electrochemical performance. Interfacial polarization resistances of a cell with the bilayer anode were 1.20, 0.49, 0.22, and 0.1 Ω cm^2 at 500, 550, 600, and 650°C, respectively, demonstrating peak power densities of 171, 301, 441, and 544 mW/cm^2, respectively.
© 2006 The Electrochemical Society. [DOI: 10.1149/1.2179189] All rights reserved.

Manuscript submitted September 13, 2005; revised manuscript received December 8, 2005.
Available electronically March 2, 2006.

Performances of solid oxide fuel cells (SOFCs) at reduced temperatures are primarily limited by the polarization resistances at the electrolde/electrolyte interfaces.[1-3] To reduce the interfacial polarization resistances, various cell configurations fabricated by different approaches have been examined.[4-7] For example, a thin intermediate CeO_2 layer between electrode and electrolyte was found beneficial to electrochemical performance of SOFCs.[8] SOFCs with electrodes fabricated by combustion chemical vapor deposition (CVD) showed higher porosity, stronger intergrain bonding, and better adhesion of electrodes to electrolyte, leading to much lower interfacial polarization resistances.[9]

It has been generally recognized that functionally graded electrodes may facilitate mass and charge transport and thus enhance electrode performance of SOFCs. To date, it appears to be easier to produce a composition-graded electrode than to create a microstructure-graded electrode, although many attempts have been made to fabricate SOFC electrodes graded in both composition and microstructure.[10-13] For example, nanostructured and functionally graded cathodes were fabricated by a combustion CVD process.[14] These electrodes were graded in composition, consisting of more material (e.g., strontium-doped lanthanum manganite, LSM) that is catalytically reactive for oxygen reduction (and compatible with the electrolyte) near the electrode/electrolyte interface and more material (e.g., strontium-doped lanthanum cobaltite, LSC) that is electronically conductive (and compatible with the interconnect) farther away from the electrode/electrolyte interface. Meanwhile, pore size variation was achieved by managing particle size at different regions of the cathode layer.

A practical strategy for tailoring porosity in SOFC electrodes is to use pore formers (e.g., graphite and cellulose), which can be removed during subsequent processing steps. Electrodes of high porosity have been created by this method for impregnation of active electrode materials.[15] When the amount of pore former is too large, however, distortion or even collapse of the intended porous structure may occur during firing because the removal temperatures of these pore formers are much lower (usually about 400–500°C) than the firing temperatures (higher than 1350°C) of the electrodes. Here we demonstrate a new method to create additional porosity in SOFC anodes using an immiscible metal oxide as a sacrificial phase. Nanoparticles of tin dioxide together with anode materials (NiO-GDC) were prepared using a combustion CVD process from a single solution containing all precursors. The pore creator, SnO_2, was then removed during firing and/or in subsequent fuel cell testing.

The design of the anode-supported cell is schematically illustrated in Fig. 1. The anode has two layers with different porosities: the bottom half layer being more porous than the upper half layer, which is in contact with the GDC electrolyte. A full cell was fabricated by copressing (bilayer anode and thin electrolyte) and screen-printing (cathode). NiO and $Gd_{0.1}Ce_{0.9}O_2$ (GDC) powder was prepared separately by glycine-nitrate process (GNP).[1] NiO powder was mixed with GDC powder in a weight ratio of 35:65 by dry-milling. Nanostructured composite powder (20 wt % SnO_2-50 wt % NiO-30 wt % GDC) was synthesized using combustion CVD from a single solution containing all precursors. To prepare the anode/electrolyte three-layer structure, the SnO_2–NiO-GDC composite powder was dry-pressed in a steel die under 100 MPa. The premixed NiO-GDC powder was then added on the top of the SnO_2–NiO-GDC composite layer and pressed at 150 MPa. Finally, an appropriate amount of GDC powder was distributed on the top and pressed at 250 MPa. The three-layer pellet was removed from the steel die and sintered in air at 1400°C for 5 h. The amount of powder for each layer was controlled to give final thicknesses of 25, 100, and 100 μm for GDC electrolyte, NiO-GDC, and SnO_2–NiO-GDC layer after sintering. Slurry consisting of $Sm_{0.5}Sr_{0.5}CoO_3$ (SSC) and 30 wt % GDC was applied to the top of the sintered GDC electrolyte by screen-printing. The cathode layer was fired at 950°C for 5 h. The detailed microstructure and phase composition of the assembled single cell were characterized using scanning electron microscopy (SEM, Hitachi S-800) and X-ray diffraction (XRD, PW-1800). The impedances and the *I-V* characteristics of the cells were measured (using Solartron SI1287 electrochemical interface coupled with SI1255 frequency response analyzer) at 500 to 650°C using humidified hydrogen as fuel and ambient air as oxidant.

The SnO_2–NiO-GDC composite powder was prepared by a combustion CVD process. Precursors containing the desired metal species were dissolved in an organic solvent. The solution was pumped into an aerosol generating nozzle and combusted with oxygen and

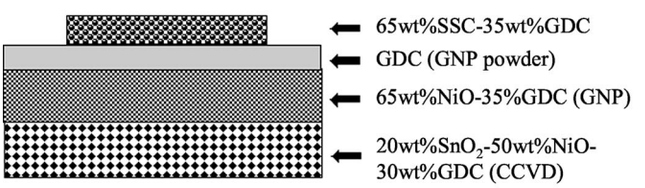

Figure 1. A schematic of anode-supported SOFC. Bilayer anode and GDC electrolyte were copressed and cosintered at 1400°C for 5 h. SSC-GDC cathode was screen-printed onto the surface of the GDC electrolyte and fired at 950°C for 5 h.

* Electrochemical Society Student Member.
** Electrochemical Society Active Member.
z E-mail: meilin.liu@mse.gatech.edu

Downloaded on 2013-05-22 to IP 128.61.137.229 address. Redistribution subject to ECS license or copyright; see ecsdl.org/site/terms_use

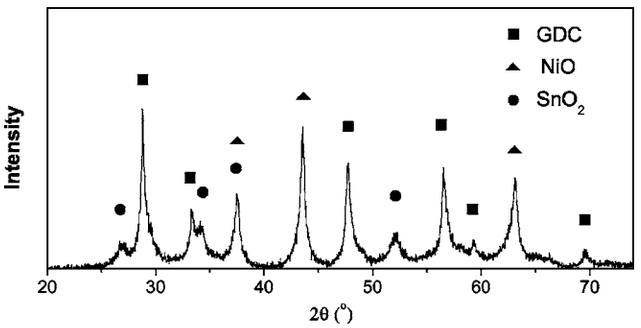

Figure 2. XRD pattern of nanocomposite powder of SnO_2–NiO–$Gd_{0.1}Ce_{0.9}O_2$ as-prepared by combustion CVD.

methane. The resulting nanopowder was collected in a specially designed device. Figure 2 shows an X-ray diffraction (XRD) pattern of the as-prepared SnO_2–NiO-GDC composite powder. Well-resolved peaks correspond to individual SnO_2, NiO, and GDC phases. There were no intermediate or undesired crystallographic phases detected from the XRD spectra.

Figure 3 shows the typical microstructures of the electrolyte and anode before and after cell testing. Shown in Fig. 3a is the GDC electrolyte and NiO-GDC interface after the copressed triple-layer pellet was sintered at 1400°C for 5 h. It can be seen that the GDC electrolyte is very dense except for a small amount of isolated voids. In the NiO-GDC anode, two distinct phases can be easily identified, dark, large NiO grains, and a light GDC phase distributed around NiO grains. The interface between the NiO-GDC and SnO_2–NiO-GDC layer is shown in Fig. 3b. It is noted that the SnO_2–NiO-GDC region has already had some porosity. This is due to the partial removal of SnO_2 nanopowder during high-temperature sintering. The melting point of bulk SnO_2 is 1630°C and the melting point for nanosized SnO_2 powder is expected to be much lower. Our experimental data indicate that the SnO_2 phase within SnO_2–NiO-GDC composite material can be completely removed at 1450°C for 5 h. After electrochemical performance testing, the sample was examined using SEM for any microstructure change. Shown in Fig. 3c is the micrograph of GDC electrolyte and NiO-GDC anode interface after cell testing at 500 to 650°C. Since NiO has been fully reduced to Ni metal, the anode material became porous. The interface between the NiO-GDC and the SnO_2–NiO-GDC layer within the anode is shown in Fig. 3d. While the entire structure is highly porous, the two anode layers of different porosity can be easily distinguished. Large voids can be seen in the NiO-GDC layer due to the irregular shape of original NiO particles. In contrast, pore size in SnO_2–NiO-GDC layer is much smaller and more uniform. The porosity of the SnO_2–NiO-GDC layer is apparently higher than that of the NiO-GDC layer.

According to theoretical calculation, there is a 33% volume reduction when NiO (6.7 g/cm^3) is reduced to Ni metal (8.9 g/cm^3). The estimated total porosity is about 27.1% in the Ni-GDC layer if full density is assumed after sintering and 40.8% in the SnO_2–NiO-GDC layer when NiO is fully reduced and SnO_2 is completely removed.

Shown in Fig. 4 is the electrochemical performance of the fuel cell. Shown in Fig. 4a are the impedance spectra measured at 500–650°C. The interfacial resistances as determined from the impedance spectra shown in Fig. 4a were 1.20, 0.49, 0.22, and

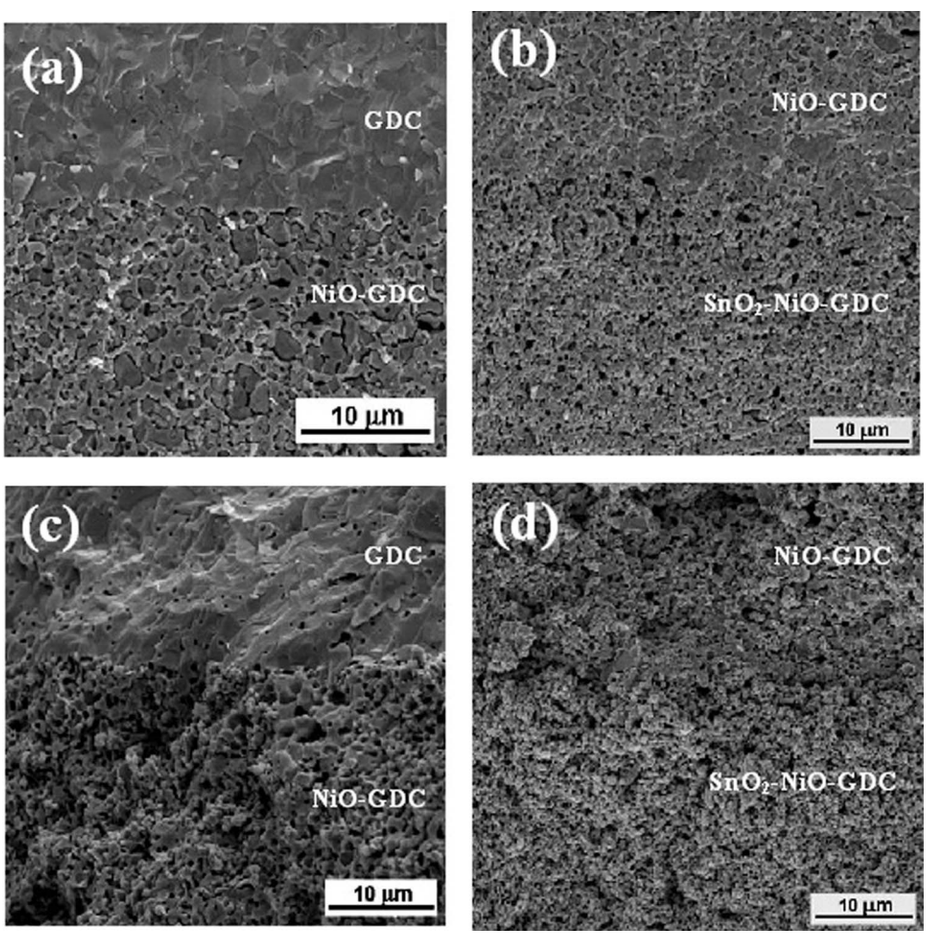

Figure 3. Cross-sectional SEM images of SOFC anode and electrolyte: (a) the interface between the GDC electrolyte and the NiO-GDC anode after sintering, (b) the interface between the NiO-GDC and the SnO_2–NiO-GDC layer after sintering, (c) the interface between the GDC electrolyte and the NiO-GDC after cell testing, and (d) the interface between the NiO-GDC and the SnO_2–NiO-GDC layer after cell testing.

Downloaded on 2013-05-22 to IP 128.61.137.229 address. Redistribution subject to ECS license or copyright; see ecsdl.org/site/terms_use

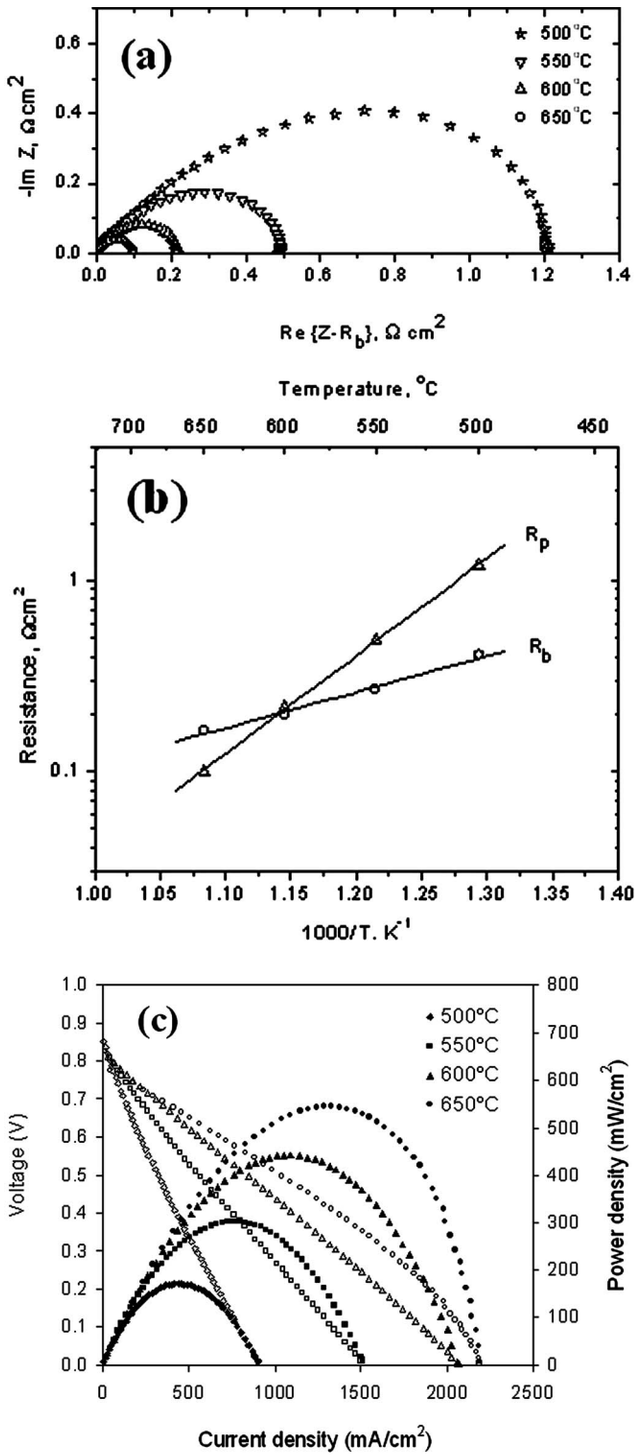

Figure 4. Electrochemical performance of a bilayer-anode-supported SOFC at 500–650°C: (a) impedance spectra of the cell (bulk resistances have been deducted), (b) Arrhenius plots of the interfacial polarization resistances (R_p) and bulk resistances (R_b) determined from impedance data, and (c) cell voltage and output power density as a function of current density passing through the cell.

0.1 Ω cm^2 at 500, 550, 600, and 650°C, respectively. The Arrhenius plots of interfacial polarization resistances (R_p) and bulk resistances (R_b) are shown in Fig. 4b. The activation energies calculated from the slopes of the Arrhenius plots are 1.02 eV (98.2 kJ/mol) for R_p and 0.37 eV (36.1 kJ/mol) for R_b. It is clear that R_b is larger than R_p at high temperatures while R_p dominates at temperatures below 600°C.

The cell voltages and power densities are shown in Fig. 4c as a function of current density passing through the cell. Peak power densities at 500, 550, 600, and 650°C are 171, 301, 441, and 544 mW/cm^2, respectively. These values are comparable to those reported in the literature.[1] It was noted that the open cell voltages (OCVs) were lower than the theoretical values; this is attributed to some electronic conduction in the GDC electrolyte[16] and some gas permeation through the seals (Ag paste) used for cell construction. For anode-supported SOFCs, mass transport of fuel gas and water vapor through the anodes may hinder the anodic processes. High porosity may help to minimize the resistance to mass transfer.

A bilayer anode supported SOFC was constructed by copressing and cosintering a bilayer anode-supported electrolyte and subsequent screen-printing of a cathode on the electrolyte. The porosity of the anode can be increased or tailored by using an immiscible metal oxide as the pore former, which will be removed during sintering or subsequent testing. Nanocomposite powder consisting of 20 wt % SnO_2-50 wt % NiO-30 wt % GDC was prepared by combustion CVD and used to demonstrate the new concept. Further, cells based on the bilayer anode of different porosities showed good electrochemical performance. This approach opens up new avenues for optimization of SOFC microstructures.

Acknowledgments

This work was supported by DOE-SECA (DE-FC26-02NT41572) and by the Center for Innovative Fuel Cell and Battery Technologies, Georgia Institute of Technology.

Georgia Institute of Technology assisted in meeting the publication costs of this article.

References

1. C. Xia and M. Liu, *Solid State Ionics*, **144**, 249 (2001).
2. S. de Souza, S. J. Visco, and L. C. De Jonghe, *Solid State Ionics*, **98**, 57 (1997).
3. S. P. Simner, J. F. Bonnett, N. L. Canfield, K. D. Meinhardt, J. P. Shelton, V. L. Sprenkle, and J. W. Stevenson, *J. Power Sources*, **113**, 1 (2003).
4. E. P. Murray, M. J. Sever, and S. A. Barnett, *Solid State Ionics*, **148**, 27 (2002).
5. V. Dusastre and J. A. Kilner, *Solid State Ionics*, **126**, 163 (1999).
6. S. P. Yoon, J. Han, S. W. Nam, T.-H. Lim, I.-H. Oh, S.-A. Hong, Y.-S. Yoo, and H. C. Lim, *J. Power Sources*, **106**, 160 (2002).
7. S. P. Jiang, S. Zhang, Y. D. Zhen, and W. Wang, *J. Am. Ceram. Soc.*, **88**, 1779 (2005).
8. Y. Matsuzaki and I. Yasuda, *Solid State Ionics*, **152–153**, 463 (2002).
9. Y. Liu, S. Zha, and M. Liu, *Adv. Mater. (Weinheim, Ger.)*, **16**, 256 (2004).
10. P. Holtappels and C. Bagger, *J. Eur. Ceram. Soc.*, **22**, 41 (2001).
11. C. Xia, W. Rauch, W. Wellborn, and M. Liu, *Electrochem. Solid-State Lett.*, **5**, A217 (2002).
12. S. Zha, Y. Zhang, and M. Liu, *Solid State Ionics*, **176**, 25 (2004).
13. N. T. Hart, N. P. Brandon, M. J. Day, and N. Lapena-Rey, *J. Power Sources*, **106**, 42 (2002).
14. Y. Liu, C. Compson, and M. Liu, *J. Power Sources*, **138**, 194 (2004).
15. R. J. Gorte and J. M. Vohs, *J. Catal.*, **216**, 477 (2003).
16. M. Liu and H. Hu, *J. Electrochem. Soc.*, **143**, L109 (1996).

Downloaded on 2013-05-22 to IP 128.61.137.229 address. Redistribution subject to ECS license or copyright; see ecsdl.org/site/terms_use